Mon. Not. R. Astron. Soc. 276, 715-722 (19

Spectral irradiance calibration in the infrared – V. The role of UKIRT and the CGS3 spectrometer

Martin Cohen[1,2] and John K. Davies[3]

[1]*Radio Astronomy Laboratory, 601 Cambell Hall, University of California, Berkeley, CA 94720, USA*
[2]*Jamieson Science and Engineering, Inc., 5321 Scotts Valley Drive, Suite 204, Scotts Valley, CA 95066, USA*
[3]*Joint Astronomy Centre, 660 N. A 'ohōkū Place, Hilo, HI 96720, USA*

Accepted 1995 April 12. Received 1995 March 15

ABSTRACT

We describe, illustrate, and quantify the performance achieved by the combination of CGS3 and UKIRT, with emphasis on the role already played by CGS3 in the field of spectrally continuous, absolute, infrared radiance calibration. The focus of the paper is on the reliability and reproducibility of the spectral shapes obtained by CGS3. We offer an electronically available data base of calibration spectra taken with UKIRT and CGS3 of a variety of infrared-bright cool K and M giants. These highlight the influence of the SiO fundamental absorption on the stellar spectra as effective temperature is varied. The calibration archive has an absolute pedigree traceable directly to Cohen et al.

Key words: techniques: spectroscopic – infrared: general.

1 INTRODUCTION

The purpose of this paper is threefold. First, we describe the role currently being fulfilled by UKIRT's CGS3 spectrometer in creating absolutely calibrated continuous infrared spectra. The key importance of CGS3 to this programme (Cohen, Walker & Witteborn 1992b) requires that its credentials be explained. Secondly, we present 7.5–13 μm spectral fragments secured with CGS3 of a wide variety of stellar spectral types in the form of the ratios of cool stellar spectra to hot stellar spectra. Thirdly, we describe an effort to calibrate these spectra absolutely using independent photometry, thereby providing an archive of calibrated CGS3 spectra, electronically available to the astronomical community for use either with CGS3 or other 10-μm instruments.

In Section 2 we briefly describe the physical attributes of the CGS3 instrument. Section 3 illustrates the actual performance achieved on UKIRT, focusing on issues of reproducibility of spectral shape as a function of time, aperture, and spectral resolution. Section 4 presents a series of ratios of stellar spectra between 7.5 and 13 μm, reinforcing the importance of the SiO fundamental absorption and its influence on normal stellar spectral energy distributions in this wavelength region (Cohen et al. 1992c) and its effects on photometry between 8 and 10 μm. Section 5 emphasizes the role of independently calibrated broad- and narrow-band photometry in normalizing spectral shapes.

We will conclude that the combination of CGS3 and UKIRT, with apertures of at least 5.5 arcsec (which is unfortunately not universal on large infrared telescopes working spectroscopically) and the routine use of an autoguider, offers an extraordinarily robust calibration tool for 10-μm spectroscopy at low (and modest) resolution.

2 A DESCRIPTION OF CGS3

CGS3 is a liquid-helium-cooled grating spectrometer which employs a linear array of 32 Si:As photoconductive detectors for spectroscopy in the 10- and 20-μm windows. A spectrum taken by CGS3 at a given grating position is sampled once per resolution element. In order to obtain full (Nyquist) or greater sampling, the number of subspectra must be two or more. Typically, double or triple sampling is used to achieve the expected resolution. Consequently, CGS3 spectra are composed of several interleaved subspectra, each of which is the average of several individual beamswitch observation pairs, each of which may have been divided by an optional sky spectrum. (Note that this implies that not all subspectra are obtained simultaneously so some minutes or even tens of minutes can intervene between acquisition of one subspectrum and the next.)

There is a rotating sector chopper, mounted on the CGS3 optical platform, which provides the instrument with alternating views through the telescope and of the ambient-temperature blackbody emission (i.e. the blades themselves).

This is used for sky-spectra, flat-fielding, and lamp spectra. Optional sky spectra are taken with the instrument set up in the same configuration that will be used to observe the astronomical source. These spectra are formed by modulating the sky's emission spectrum with the chopper, so are strictly only true sky spectra if the sky column is at the same temperature as the chopper blade.

Beamswitching and the taking of sky and source spectra are all done automatically. Sky division, if used, approximately removes the detector array's flat-field response and eliminates the gross effects of variations in sky transmission with wavelength. It is ideally used in addition to the division of the spectrum by a standard star (which has also been divided by the sky). Aperture diameters range from 1.5 to 9 arcsec. Three gratings are available in the spectrometer, and provide coverage and resolutions as listed in Table 1 for measurements made in the nominal 5.5-arcsec aperture (5.5 arcsec FW at 10 per cent, 4.8 arcsec FWHM). The spectral profile of CGS3 is roughly rectangular. Fig. 1 illustrates two orthogonal scans of the spatial profile of the 5.5-arcsec aperture in CGS3 to demonstrate the flat-topped character of the beam profiles.

The longer process of integrating on-source then begins, with the telescope chopping from source to nearby blank sky at the chop frequency, then nodding to remove thermal offsets between the two beams every dwell-time period (typically 10 s). For each beamswitch pair the coadded source spectrum divided by the sky is plotted for the observer to see. This spectrum is known as a 'subspectrum'. In order to produce a final spectrum that is fully sampled in wavelength, it is necessary to interleave several subspectra taken at nearby grating positions, and so the steps above are repeated at least once to produce the final observation.

Wavelength calibration is accomplished by observing high orders of the dominant line of Krypton at 2.1908 μm. For use with a 10-μm grating, the fourth, fifth, and sixth orders of this line at 8.763, 10.954, and 13.145 μm are useful; if the 20-μm grating is selected, a strong line will be seen in ninth order at 19.72 μm, flanked by about four other weaker lines.

3 THE ACTUAL PERFORMANCE OF CGS3 ON THE UKIRT

The critical issue for any spectrometer is whether it delivers the correct shape of a spectrum. Because it can be used with a variety of apertures, and because smaller apertures mean less background and hence greater sensitivity, users are apt to use spectrometers with apertures too small to assure spectrophotometric accuracy, according to accepted views. The danger in spectroscopy is that too small an aperture will preferentially shed light at the longer wavelengths where the Airy disc is significantly larger than at the shorter wavelengths on the CGS3 gratings. This leads to a tilt in the slope of the spectrum obtained. We encourage the use of at least the 5.5-arcsec aperture with CGS3, which is also approximately the beamsize used with the UKIRT bolometer (UKT8) system.

In the scheme recommended in Cohen et al. (1992b), one demands only that a spectrometer yields an accurate shape, albeit for the ratio of two spectra, not necessarily absolutely accurate photometric signals at each wavelength. How closely does CGS3 achieve this primary requirement, as a function of several pertinent variables: (1) stability and reproducibility on short and long time-scales; (2) spectral resolution; and (3) aperture? Secondly, how closely can CGS3 approach precise radiometric accuracy in these spectral ratios?

3.1 Reproducibility

The model of operation is to set the grating to the first required position, acquire all necessary 'subspectra', then move the grating and repeat this procedure for the one or two remaining grating settings. Note that the separate grating settings result in raw data files that are interlaced in wave-

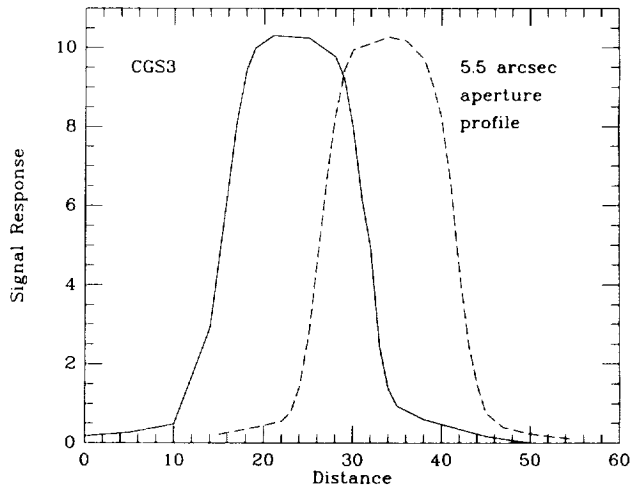

Figure 1. Two orthogonal cuts through the 5.5-arcsec CGS3 aperture to show the beam profiles. 5.5 arcsec represents the FW at 10 per cent intensity of the flat-topped profiles.

Table 1. Gratings and resolutions available with CGS3.

Grating Name ruling	Available Wavelengths μm	Spectral range μm	Optimum Filter μm	Detector spacing μm	Resolution FWHM μm	Sensitivity 1σ 1 sec		
						mag	Jy	W m^{-2}
HIRES_10 105 l mm^{-1}	7–15	1.6	7–22	0.05	0.060	2.3	5.0	0.8×10^{-14}
LORES_10 35 l mm^{-1}	7–15	5.8	7–22	0.19	0.20	3.0	2.5	1.5×10^{-14}
20 25 l mm^{-1}	16–24	8.3	15–24	0.27	0.275	0.4	7.0	1.6×10^{-14}

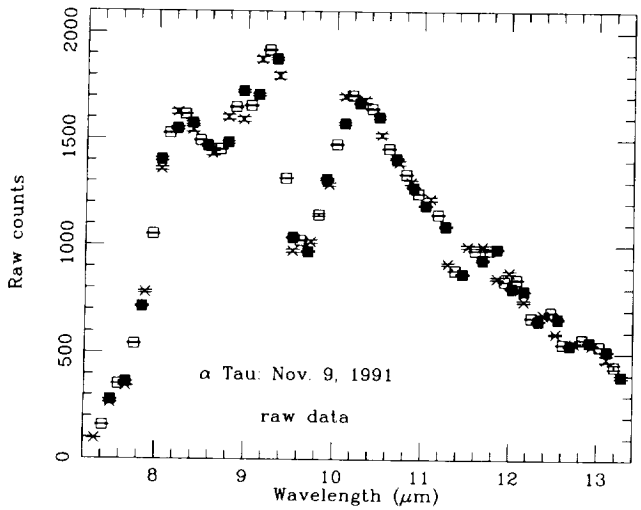

Figure 2. Raw counts from three separate subspectra of α Tau taken consecutively on 1991 November 9. 1 σ error bars are plotted but are generally smaller than the symbols used to denote the data points.

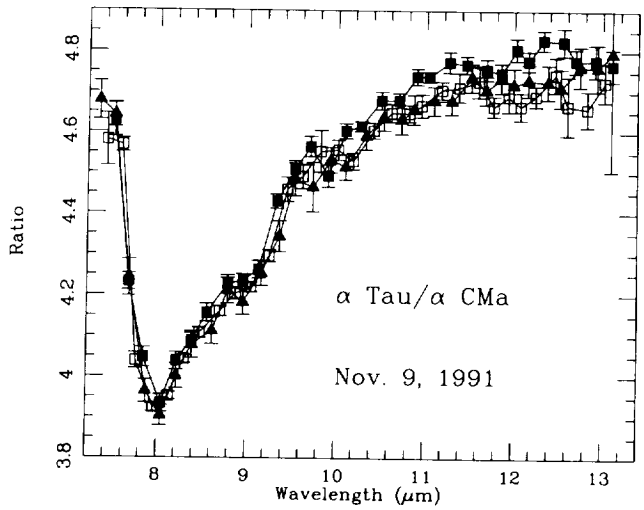

Figure 3. Ratios of raw counts of α Tau and α CMa from three pairs of consecutive subspectra on 1991 November 9 with matched airmasses. Note the very close accord of these unadjusted low-resolution spectral ratios. 1 σ error bars are plotted.

length, each covering identical total ranges, with wavelength scales offset by $\frac{1}{3}$ (or $\frac{1}{2}$ in double sampling mode) of a resolution element. If all is stable instrumentally (including the guiding, a most critical item in the overall system), the sky stability and seeing are good, and the aperture is not too small, then these consecutively taken, independent raw spectra should be interlaced perfectly. Fig. 2 illustrates this for three spectra of α Tau (taken 1991 November 9 with a 5.5-arcsec aperture). The same shape is conspicuously well reproduced by all three independent spectra and the total spread between the three raw spectral shapes is ~0.7 per cent.

An even more demanding criterion is to compare the three *ratios* of spectra of two stars, obtained from the three distinct pairs of subspectra. Fig. 3 illustrates this more rigorous test in the case of ratios of α Tau to α CMa, also from 1991 November 9, again in the 10-μm window, at low resolution. Airmasses (AMs) of the two stars were deliberately well matched to have a difference in AM < 0.02. These three interlaced ratio subspectra have not been adjusted in any way, yet all match within 3 per cent, even at the longest wavelengths. This tests stability and fidelity of spectral shape on two short time-scales: that associated with a single grating setting on these bright stars (about 2–5 min); and that within a night, on a scale of a few hours.

Fig. 4 examines reproducibility on a night-to-night time-scale using an aperture with an even smaller diameter. We present this figure for two reasons. First, it is indicative of those places in a 10-μm spectrum where unmatched airmasses can give rise to specious structure; it speaks eloquently of the need to take great care in scheduling observations unless one is willing post facto to remove atmospheric features arising from differential airmass using an appropriate code [e.g. FASTCODE (Rothman et al. 1987); or IRTRANS (Traub & Stier 1976)]. Secondly, outside those regions contaminated by time-varying water vapour (below about 8.2 μm) and ozone (roughly 9.3–9.8 μm), note the match both of shape and level between these spectral ratios of β Gem to α Tau obtained on 1993 November 4 and 1993 November 5

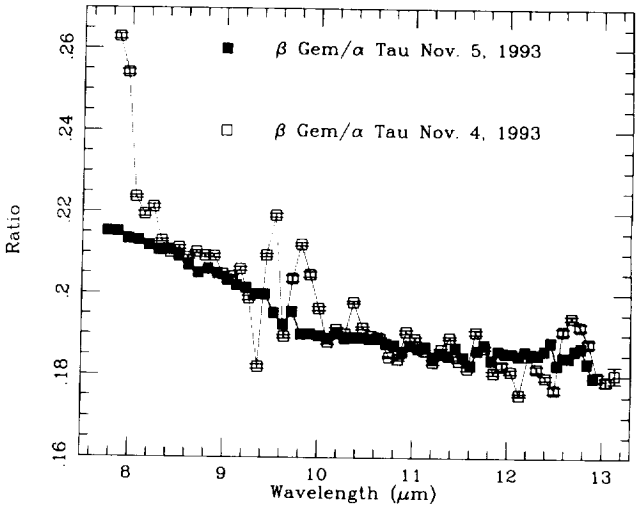

Figure 4. Ratios of raw counts of β Gem and α Tau taken on two consecutive nights in 1993 November. 1 σ error bars are plotted. Observations on November 5 were closely matched in airmass; those on November 4 were not. Note the effects at the band edge below 8.2 μm, where telluric water vapour enters, and in the ozone between 9.3 and 9.9 μm.

with only 3.3-arcsec apertures throughout. Shape and level agree to better than about 2.5 per cent except near 13 μm where the difference rises to some 6 per cent. The airmasses were perfectly matched on November 5, but differed by about 0.3 airmass on November 4. We feel that the lack of airmass match on the earlier spectral pair has caused not only spurious spectral 'features' but also any wavelength-dependent differences in spectral shape between the ratio spectra. The enhanced level of noise on November 4 also betrays the difference of airmass. Of course, we note that, while airmass matching is clearly important, atmospheric changes within a night (in transparency, or water vapour) can invalidate even an airmass-matched ratio of stellar spectra.

3.2 Aperture effects

Fig. 5 investigates the effects of defining spectral ratios using different aperture measurements to secure the same ratios of α Tau to α CMa taken at low resolution on 1991 November 9 (triply sampled) and 1993 November 7 (doubly sampled this time). The actual levels of the ratio spectra are well reproduced (within 4.4 per cent). The shapes are in excellent agreement, as shown in Fig. 6, where the 1991 data are compared with those from 1993 rescaled by 0.958 (the best-fitting matching of the levels). Differences in shape are generally <2 per cent, rising to 3.2 per cent at the longest wavelengths. We emphasize that in each of these sets of observations: (1) great care was taken to match airmasses of the two stars closely; and (2) an autoguider was used throughout to supply objective and high-frequency guiding of the stellar images. Apertures used were 5.5 arcsec in 1991 but only 3.3 arcsec in 1993. Shape is clearly very well reproduced but radiometric level has suffered at the roughly 5 per cent level. The 1993 data show a higher level in raw spectral ratio which we attribute to signal from Sirius (in this case the fainter star) being preferentially lost due to effects of seeing, guiding, etc. We stress, however, that we would not be surprised to see this raw ratio show the inverse behaviour, so dependent is it upon differential external conditions (seeing, haze, transmission) for the several independent data sets required. Incidentally, this good agreement also provides an end-to-end test of CGS3 on the long term (years) time-scale, showing that no instrumental effects have varied (e.g., the individual detectors' responsivities as a function of background) to the point where short-term ratios of spectra cannot remove them.

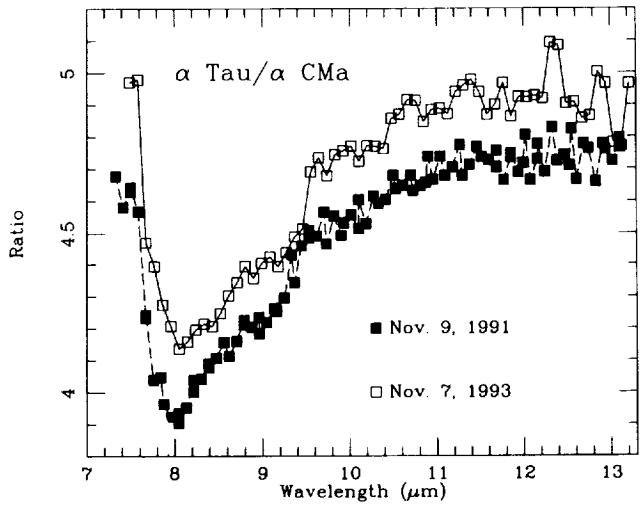

Figure 5. Ratios of low-resolution merged subspectra of α Tau and α CMa taken with different apertures, but each with matched airmasses. The 1991 data are triply sampled with 5.5-arcsec aperture; those of 1993 are doubly sampled with only 3.3-arcsec aperture. Note that the shapes are extremely well reproduced and the actual levels are only about 4 per cent different.

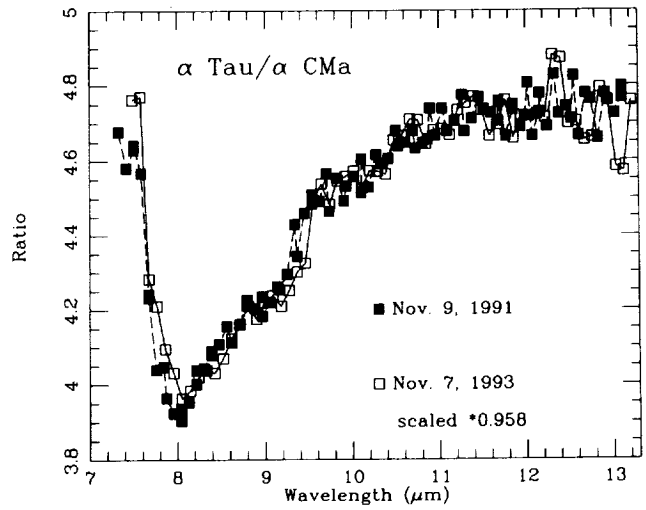

Figure 6. As in Fig. 5, but after merging the 1991 ratio with the 1993 observations, rescaled by the best-fitting factor of 0.958 to the 1991 spectrum. These observations illustrate what can be expected if one uses different apertures in CGS3.

Very recently, a theoretical analysis was carried out to determine the effect of aperture size on the calibration of CGS3, taking into account the influence on the Airy pattern of the central obscuration in the telescope. This report (Rees 1994) concludes that, at 10 μm, the 3.3-arcsec aperture so popular for spectroscopy of faint objects cannot include more than 95 per cent of the total light, whereas the 5.5-arcsec diameter aperture we use with CGS3 on UKIRT attains ~97 per cent. Rees also demonstrates that there is an effect on spectral shape such that systematically more light is lost at shorter wavelengths, leading to a spectral curvature. For these two apertures, the magnitude of this change in spectral shape across the whole range from 7.5 to 13 μm is ~3 per cent. This analysis pertains to ideal conditions, when the qualitative phenomenon is a sharpening of the Airy disc with a simultaneous translation of energy outwards into the diffraction pattern, so the contrast between peak and rings is diminished. Under real seeing conditions, however, there is already softening of the ideal diffraction pattern and one might expect the actual spectral curvature to be less than estimated above. Likewise, any such wavelength-dependent effects are removed or at least greatly reduced by dividing one stellar spectrum by another. Only the differential light loss with wavelength remains, as a consequence of the potentially different seeing conditions under which the two stars were observed. There is, of course, no doubt that smaller apertures are still appreciably less capable of including all the light available in a CGS3 spectrum than are larger apertures.

3.3 Spectral resolution

During these 1991 November observations, both low- and high-resolution spectra of α Tau and α CMa were secured with CGS3. Apertures were 5.5 arcsec throughout the night which was clear, dry and calm. Airmasses were matched closely, though more closely on the low-resolution pair due to the rigours of meeting all the detailed demands of scheduling, so that these observations could serve as an unambiguous demonstration of what can be attained with sufficient care. Fig. 7 presents the raw ratios of spectra, α Tau/α CMa, distinguishing high from low resolution. Note the faithful reproduction of shape (a handful of discrepant points are

identifiable in the ozone region because the higher-resolution data sample the same terrestrial ozone lines more sharply than the low and were not so well matched in airmass as the low). The raw ratio levels differ by only 3.5 per cent, again probably due to differential sky conditions from star to star. When rescaling the high-resolution data by a factor of 1.035, they merge well with the low-resolution data (Fig. 8), allowing for the better signal-to-noise ratios of the low-resolution data.

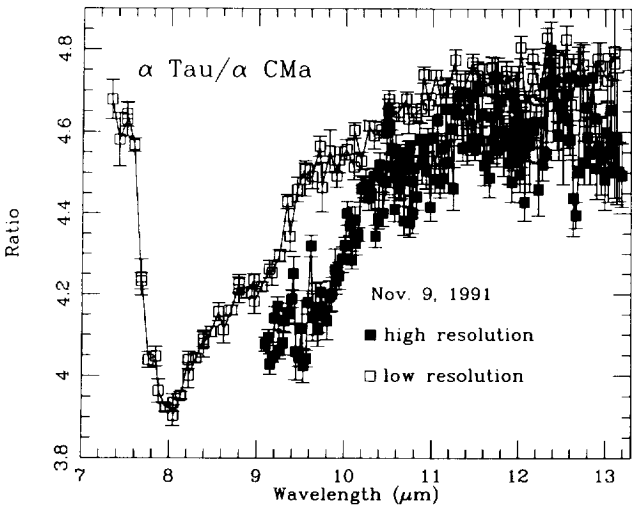

Figure 7. Comparison of low- and high-resolution spectral ratios of α Tau and α CMa on 1991 November 9. The low-resolution data represent triply sampled subspectra; those at high resolution correspond to three separate grating settings, each double sampled, all merged by the same techniques described by Cohen, Walker & Witteborn (1992b). The two sets of unadjusted spectral ratios are only 3.5 per cent apart. 1 σ error bars in the ratios are plotted.

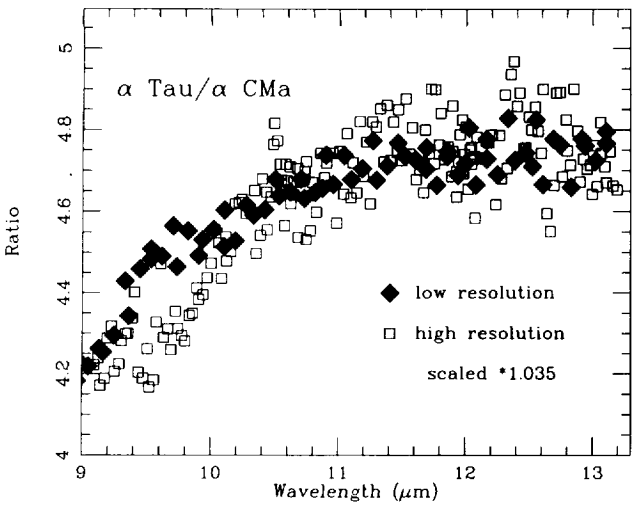

Figure 8. As in Fig. 7 but after merging the low- and high-resolution observations, and after rescaling the latter by the best-fitting factor of 1.035 to the low-resolution spectrum. Note the excellent agreement between the two spectra, except in the ozone region (~ 9.3–9.8 μm). The high-resolution observations were not matched quite as closely in airmass as the low.

4 SPECTRAL TYPE AND MOLECULAR FEATURES

The stars selected for discussion and for building the archive of calibrated spectra are all 'normal', without dust shells, and not of extreme luminosity or metal abundance. Table 2 summarizes the details of the spectra taken of these selected stars whose ratios with respect to either Vega or Sirius are presented in Fig. 9. These were constructed from the products of the ratios in Table 2 (possibly combined to enhance the signal-to-noise ratio when more than one ratio is available for a given star) with 'basic' ratios such as α Tau/α CMa and α Boo/α Lyr, because one cannot always take a spectrum of either Vega or Sirius on a particular night, and because higher signal-to-noise spectra always result from comparisons with infrared-bright comparison stars like α Tau or α Boo. When there are a few discrepant points at wavelengths that suffer from the greatest sensitivity to time variations in ozone or water vapour, these have been omitted from the individual plots. This can occur in products of spectral ratios even when the separate component ratio spectra already involve close airmass matching. The product of spectra can effectively amplify any slight mismatches in telluric molecular absorptions. These effects are not, however, detrimental in any way to the bulk of the points in a spectrum (see Section 3.1), and are confined to a handful of points either at the shortest, or longest, wavelengths or near the 9.6-μm ozone feature.

We have attempted to show spectra in Fig. 9 that span a significant range of spectral types although there is essentially no low-resolution spectral content of interest until late G-K0 giant types. Note the featureless nature of the hot stellar spectra (e.g. α Aql), and the growth of the P-branch of the SiO fundamental absorption (deepest at our low resolution near 7.9 μm in ratio plots) with lateness of spectral type. In Fig. 10 we have attempted to quantify the dependence of the SiO fundamental depth on spectral type (cf. Cohen et al. 1992c) by plotting the strength of the absorption near 7.9 μm relative to a reference level in the continuum. Ideally we would combine airborne 5–9 μm spectra with the CGS3 data to construct continuous 5–13 μm spectra, from which we could derive an interpolated continuum also at 7.9 μm. In the absence of airborne data for most of the stars in Fig. 9, we have, however, chosen to assess the relevant continuum based on the approximate mean level of the spectral ratios in the 11–13 μm range. Such a choice also obviates any dependence on those points most vulnerable to problems with telluric water, below 8 μm. The resulting deficits near 7.9 μm are attributed to SiO absorption and should coarsely assess the real strengths of this band in our stars. Fig. 10 also includes estimated errors in these strengths. All stars are of luminosity class III except for α Hya and β Peg, which have class 'II–III' and are distinguished by open squares in the figure. The SiO feature grows essentially linearly for the class III giants, reaching a maximum between K5III and M0III, beyond which it remains constant, as if saturation has occurred in these cool atmospheres. We can find no clear evidence for its presence in stars earlier than K0III. A similar trend was found by Rinsland & Wing who observed the first overtone bandheads in a number of late-type stars (Rinsland & Wing 1982). The spectrum of α Aur (G5III + G0III) plays a pivotal role in this pattern because the absence of recogniz-

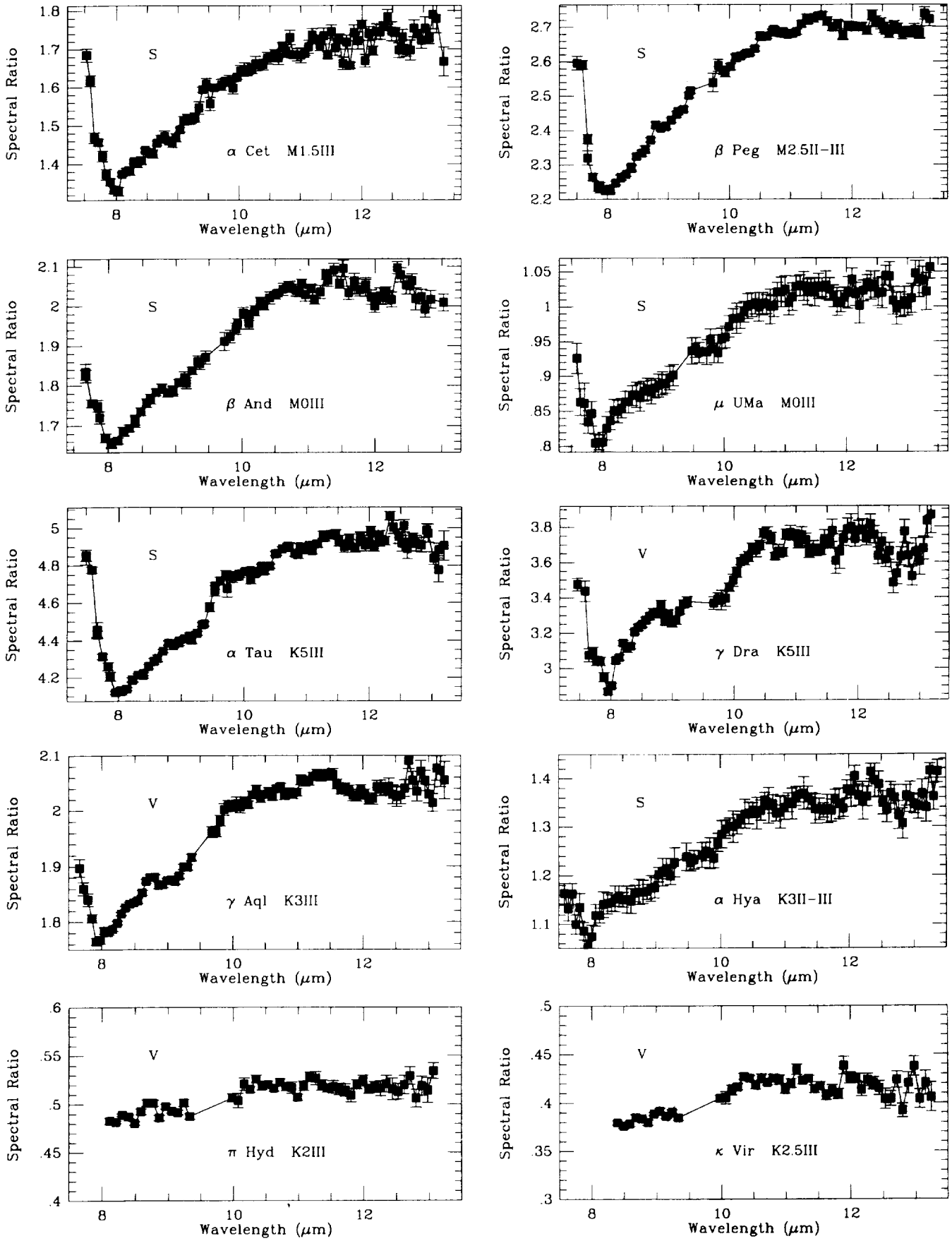

Figure 9. Montage of ratio spectra from CGS3 comparing stars with either Vega or Sirius. Each plot carries labels that indicate the star, spectral type, and reference star (the latter by the single-letter code 'V' for Vega, 'S' for Sirius in the upper-left corner).

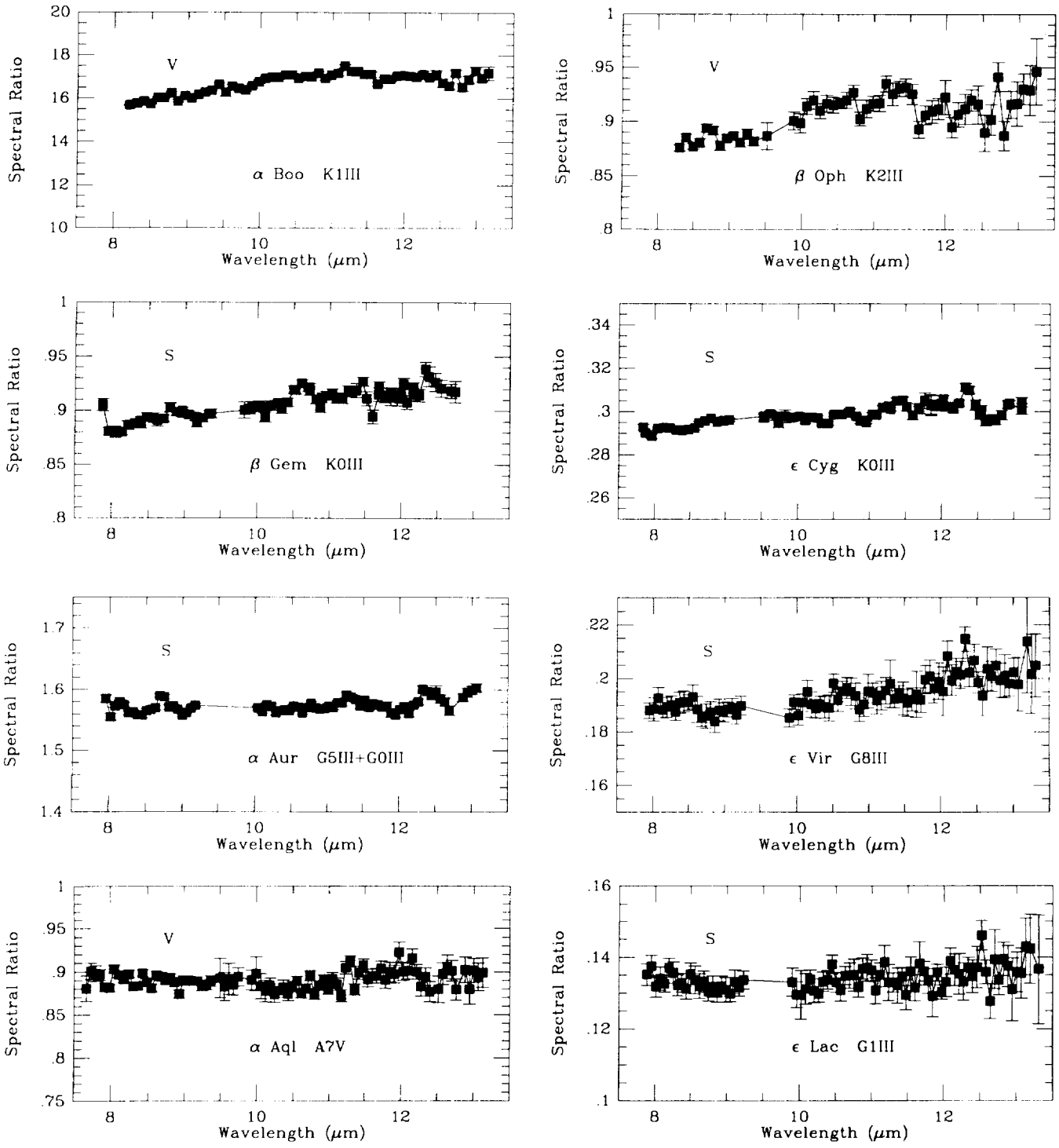

Figure 9 - *continued*

able SiO absorption in this star rules out measurable SiO absorption in typical middle and early G giants.

5 THE ABSOLUTELY CALIBRATED PRODUCTS

It is quite straightforward, given the ratios of stellar spectra to those of Vega and Sirius, to proceed from Fig. 9 to absolutely calibrated stellar spectra. We require only two procedures. First, we multiply the ratio spectra by the absolutely calibrated Vega or Sirius spectra in Cohen et al. (1992a), after smoothing the latter to match the instrumental resolution actually achieved by CGS3. Secondly, we integrate narrowband filters in the 10-μm region, with known cold transmission profiles, over the resulting 'fluxed' spectra, including the effects of the (mean) atmosphere for Mauna

Table 2. Selected stars observed with CGS3 and absolutely calibrated.

STAR	Spectral type	AM	Reference	AM	Date	Sampling
α Aql	A7V	1.03	α Lyr	1.06	May 13, 1994	3
α Aql	A7V	1.16	α Lyr	1.09	Nov. 3, 1993	2
ε Leo	G1III	1.00	α CMa	1.26	Feb. 9, 1993	3
α Aur	G5III+G0III	1.17	α CMa	1.44	Oct. 4, 1992	2
α Aur	G5III+G0III	1.17	α Tau	1.09	Aug. 29, 1993	2
ε Vir	G8IIIab	1.02	α CMa	1.26	Feb. 9, 1993	3
β Gem	K0III	1.15	α Tau	1.14	Nov. 5, 1993	2
ε Cyg	K0III	1.23	α CMa	1.24	Nov. 7, 1993	2
α Boo	K1III	1.51	α Lyr	1.75	May 29, 1991	2
β Oph	K2III	1.75	α Lyr	1.75	May 29, 1991	2
β Oph	K2III	1.51	α Boo	1.51	May 29, 1991	2
π Hyd	K2III	1.54	α Boo	1.51	May 29, 1991	2
κ Vir	K2.5III	1.01	α Boo	1.06	May 29, 1991	2
κ Vir	K2.5III	1.51	α Boo	1.51	May 29, 1991	2
γ Aql	K3III	1.75	α Lyr	1.75	May 29, 1991	2
γ Aql	K3III	1.16	α Boo	1.17	May 29, 1991	2
γ Aql	K3III	1.07	α Lyr	1.06	May 13, 1994	3
α Hya	K3II	1.26	α CMa	1.26	Feb. 9, 1993	3
α Tau	K5III	1.22	α CMa	1.25	Nov. 9, 1991	3
α Tau	K5III	1.20	α CMa	1.24	Nov. 7, 1993	2
γ Dra	K5III	1.17	α Lyr	1.09	Aug. 26, 1994	3
β And	M0III	1.08	α Tau	1.09	Aug. 29, 1993	3
μ UMa	M0III	1.25	α CMa	1.26	Feb. 9, 1993	3
α Cet	M1.5III	1.32	α CMa	1.28	Nov. 3, 1993	3
β Peg	M2.5II-III	1.01	α Tau	1.12	Oct. 5, 1990	2

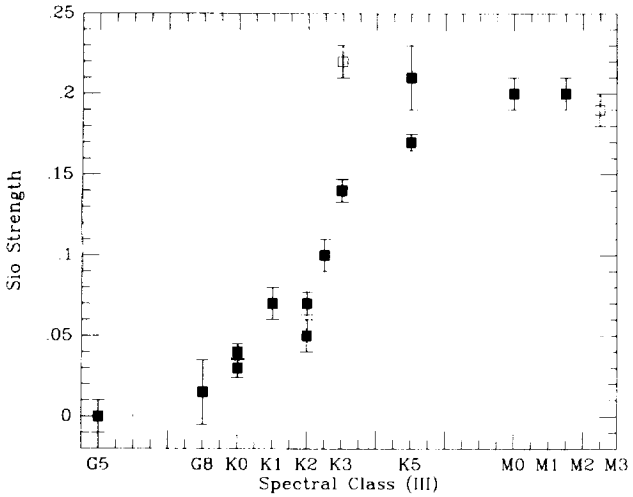

Figure 10. A coarse measure of the strength of the SiO fundamental absorption in middle G to early M giants. Solid squares represent stars of class III; open squares those of class II–III.

Kea (cf. Cohen et al. 1992a). The in-band fluxes of the stellar spectrum are then best matched to the in-band fluxes expected, given the star's magnitudes. We prefer to carry out this procedure using the UKIRT 8.7- and 11.7-μm filters, cold characterized and calibrated by Cohen et al. (1992a), rather than through use of the very broad N passband. The N filter extends to longer wavelengths than those offered by typical CGS3 grating settings; also, the signal-to-noise ratio spectroscopically is rather poor beyond 13.3 μm compared with shorter wavelengths. Further, having two passbands to satisfy provides an estimate of uncertainty beyond that of just the photometry measurement (cf. Cohen et al. 1992b).

As we secure these photometric measurements we will be able to calibrate our CGS3 spectra absolutely and such products can be obtained by e-mail to JKD at the Joint Astronomy Centre, Hawaii. We note that this procedure is precisely that detailed by Cohen et al. (1992b). Therefore, given the central role of the CGS3 10-μm spectral fragments in the entire process of assembling a complete 1.2–35 μm spectrum, the same absolute calibration results whether we treat the CGS3 fragment in isolation (as in the present paper) or abstract it from an already generated complete spectrum. This ensures consistency of the CGS3 calibration archive and the archive of complete spectra (which, of necessity, involves a much smaller set of stars than treated here because of the requirement for continuous 1–5.5 and 5–9 μm spectral fragments). We have considered using *IRAS* flux densities in the 12-μm band but the relevant system response spans a wavelength range greater than that available from the CGS3 spectra. Consequently, in the absence of photometry through characterized narrow passbands, we can provide stellar spectra whose shape is reliable but whose radiometric level is uncertain at the level of at least a few to 10 per cent.

ACKNOWLEDGMENTS

MC thanks US Air Force Phillips Laboratory for partial support of this work through Dr S. D. Price under contract number F19628-92-C-0090 with Jamieson Science and Engineering, Inc. MC also thanks NASA-Ames for partial support under cooperative agreement NGCC 2-142 with UC Berkeley. We thank Dr Tom Geballe for providing many of the excellent CGS3 spectra obtained under the Service programme and contained in the UKIRT archives, for his comments and insight on the manuscript, and Drs A. J. Adamson, M. J. Barlow, M. Hanner and Mr C. Dudley who kindly made observations available to us and encouraged us in this effort.

REFERENCES

Cohen M., Walker R. G., Barlow M. J., Deacon J. R., 1992a, AJ, 104, 1650
Cohen M., Walker R. G., Witteborn F. C., 1992b, AJ, 104, 2030
Cohen M., Witteborn F. C., Carbon D. F., Augason G. C., Wooden D., Bregman J., Goorvitch D., 1992c, AJ, 104, 2045
Rees N., 1994, report to the Science and Engineering Research Council, UKIRT Upgrades Project (1994 November 20)
Rinsland C. P., Wing R. F., 1982, ApJ, 262, 201
Rothman L. S. et al., 1987, Appl. Opt., 26, 4058
Traub W. A., Stier M. T., 1976, Appl. Opt., 15, 364